IMPROVING ENERGETIC PARTICLE CONFINEMENT IN STELLARATOR REACTORS

A. BADER, C.C. HEGNA, B. J. FABER, D.T. ANDERSON
University of Wisconsin-Madison
Madison, WI, USA
Email: abader@engr.wisc.edu

M. DREVLAK, S. HENNEBERG
Max-Planck institute for Plasmaphysics
Greifswald, Germany

Y. SUZUKI
National Institute for Fusion Science
Toki, Japan

J.C. SCHMITT
Auburn University
Auburn, AL, USA

Abstract

Calculations of alpha particle losses in various reactor-scale stellarator configurations are presented. Configurations are scaled to have plasma volume and magnetic field strength similar to the ARIES-CS reactor design. Both collisional and collisionless calculations are performed. The importance of the neoclassical metric, Γ_c, is discussed. Quasi-helically symmetric configurations are found to strongly outperform other configurations in collisionless Monte Carlo simulations. However, the performance gap narrows significantly when collisions are included. Analysis and possible explanations for the difference in relative performance is presented.

1. INTRODUCTION

Confining energetic particles, especially the alpha particles that are born in nuclear fusion reactions, is of key importance for magnetic confinement fusion reactors. In configurations where axisymmetry is not present, either tokamaks with non-axisymmetric perturbations, or stellarators, some particle orbits will have a non-zero bounce-averaged radial drift which causes them to leave the confined region, sometimes very quickly [1]. Promptly lost particles can cause significant damage to plasma facing surfaces and reduce the lifetime of the plasma wall. It will never be possible to confine all alpha particles in a fusion device, but reducing the losses, especially prompt losses, is of key importance for the longevity of the device. This paper will show collisional energetic particle transport results from various stellarator configurations at the reactor scale with the goal of identifying the properties of configurations with good confinement.

Several metrics have been developed for neo-classical confinement in 3D systems. Some configurations have contours $|\boldsymbol{B}|$ that are isomorphic to axisymmetric systems. These configurations are called quasi-symmetric, because they possess a symmetry similar to an axisymmetric system. This paper includes configurations of two quasi-symmetric types, quasi-axisymmetric where magnetic contours connect toroidally, and quasi-helical where contours connect helically. In all the configurations strict isomorphism is not present, but rather an approximate isomorphism exists. The deviation from a strict isomorphism is referred to in this paper as quasi-symmetric deviation. Mathematically this is obtained by transforming coordinates into the Boozer coordinate system [2], and then calculating the energy in the non-symmetric modes.

It has been shown experimentally that quasi-helical configurations improve neoclassical confinement [3]. Many numerical explorations of quasisymmetric configurations of all types exist as well. Specifically, recent results indicate that low quasi-symmetric deviation can help alpha confinement in both quasi-axisymmetric [4] and quasi-helically symmetric configurations [5].

Another metric, ε_{eff}, the coefficient of the neoclassical diffusion in the low-collisionality regime, has been regularly used for stellarator optimization [1]. However, recent results indicate that there is little correlation between ε_{eff} and good energetic particle confinement. However, a different metric that seeks to align contours of

the second adiabatic invariant with flux surfaces, Γ_c has had more predictive success, and has been used to optimize quasi-helically symmetric configurations with good energetic particle confinement [5,6].

The layout of this paper is as follows. In Section 2, we will briefly describe the configurations used in this paper. Section 3 will explain how the reactor scale configurations were constructed. Section 4 will show results from collisional calculations of alpha particles. Section 5 will discuss the results and describe some of the limitations of the approach. Section 6 will conclude.

2. CONFIGURATIONS

This paper considers three quasi-helically symmetric configurations, three axisymmetric configurations, a W7-X like configuration, and two LHD-like configurations. An ITER configuration is included for comparison. A table of all the configurations and their relevant properties has been included below.

TABLE 1. CONFIGURATION PARAMETERS

Name	Type	Periods	Aspect ratio	β
Wistell-A	QH	4	6.7	Vacuum
Wistell-B	QH	5	6.6	Vacuum
Ku5	QH	4	10.0	10.0%
ARIES-CS	QA	3	4.5	4.0%
NCSX	QA	3	4.4	4.3%
Henneberg	QA	2	3.4	3.5%
W7-X	QO	5	10.5	4.4%
LHD standard	Heliotron	10	6.5	Vacuum
LHD inward	Heliotron	10	6.2	Vacuum
ITER	Tokamak	N/A	2.5	2.2%

The quasi-helically symmetric configurations are: the "Wistell-A" configuration which has been described in a previous publication [7]; the "Wistell-B" configuration, a five-field period configuration optimized explicitly for energetic particle confinement; "Ku4" a four field period configuration from [8] optimized for quasi-symmetry. The three quasi-axisymmetric configurations are comprised of the NCSX [9] and ARIES-CS [10] configurations which are both well known, and a more recent configurations optimized by Henneberg et al [11]. The W7-X like configuration that is used is one designed for improved energetic particle confinement [12]. The two LHD configurations are both vacuum configurations, one is the standard configuration and the other in an inward shifted configuration which is known to have improved confinement properties [13]. Finally, the ITER configuration is a near-axisymmetric configuration, although this equilibrium includes the effects from coil ripple, blanket modules and ferritic inserts [14].

3. SCALING TO REACTOR SIZE

In order to properly scale configurations to each other it is necessary to adjust the sizes. Parameters for the ARIES-CS parameters are used for the scaling. There are two possible ways to scale the configurations. One option is to scale the configurations so that they have the same volume (450 m^3) the other option is to scale the minor radii to all be the same value (1.7 m). For this paper we only show results from the volume scaling, although the main conclusions do not change when the configurations are scaled to have equivalent minor radii.

All configurations are represented by VMEC equilibria [15], and the size scaling is accomplished by adjusting the boundary coefficients such that all configurations have the same volume. The magnetic field strengths are made equivalent by ensuring the volume averaged magnetic field is equivalent across all configurations. For non-vacuum configurations, the rotational transforms are adjusted for each configuration by using $I \propto RB$, where I is the total current in the plasma. The normalized pressure, β is similarly kept constant through the scaling procedure.

In order to perform the collisional calculations, it is necessary to define the temperature and density profiles. While the transport properties for each of these configurations are different, for the sake of this calculation the same density and pressure profiles are used throughout. No effort is made to calculate self-consistent profiles

from alpha heating. Such calculations are left for future work. The density profile is mostly flat with $n = n_0(1\text{-}s^5)$, the temperature profile is more peaked with $T - T_0(1\text{-}s)$. In the previous equations, s represents the normalized toroidal flux. The values of the core temperatures, T_0 and n_0 are approximately equivalent to those of ARIES-CS at $2.25*10^{20}$ m^{-3} and 11 keV respectively. Once the temperature profiles are chosen, the reaction profile is determined. The temperature, density and reaction profiles are shown in figure 1.

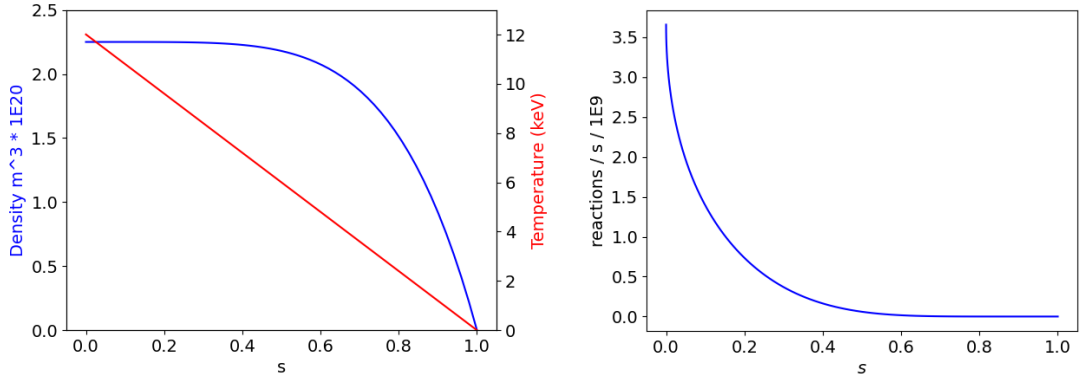

Figure 1: Left: density and temperature profiles with respect to normalized toroidal flux. Right: Reactions per second as a function of normalized toroidal flux.

4. CALCULATIONS OF ALPHA PARTICLE CONFINEMENT

Particles are sourced by first choosing a radial location such that the distribution matches the reaction profile given previously. Next a random location on the surface and a pitch is chosen in the same manner as described in [5]. The guiding centers of the particles are followed and can undergo both slowing down and pitch angle scattering. If a particle passes beyond the penultimate flux surface at any point in time it is considered lost. If the particle's energy is the same as the background thermal particle it is considered confined and is no longer followed.

The results from the collisional calculation are shown in Figure 2. The line style indicates the configuration type, with solid lines indicating QH, dotted lines QA, dashed lines for the LHD-like configurations and both ITER and W7-X use dashed-dotted lines. Among the quasisymmetric configuration, the QHs strongly outperform the QAs. The two best configurations shown (outside of ITER) are QHs. W7-X performs about equivalently to the WISTELL-A configuration and the inward shifted LHD configuration. This result will be discussed in detail later. Note that due to differences in machine size, magnetic field, and particle sourcing, the results shown here may differ from previously published results on energetic particle confinement.

Figure 3 shows the total energy loss for each configuration plotted against the minimum value of a parameter of interest, either the deviation from quasi-symmetry (for the QS configurations) in figure 3(left), or Γc in figure 3(right).

Among the QA configurations the best performing configuration is the Henneberg QA, which also performs the best on both metrics. Interestingly ARIES-CS has a larger deviation from quasisymmetry but performs better in both Γc and energetic particle confinement. The optimization of ARIES-CS explicitly degraded quasi-symmetry in order to improve confinement [16]. Even though the Γc metric had not been included the optimization of ARIES-CS, the procedure did manage to improve it significantly.

The QH configurations include the two stellarator configurations with the best confinement. For the QH configurations, Wistell-A performs worse in the quasisymmetry metric but approximately as well in Γ_c. Both Wistell-A and Wistell-B were optimized including both quasi-symmetry and Γ_c in the target function. The Ku5 configuration only optimized for quasisymmetry, but despite this has the lowest Γ_c. There is a caveat to the performances of the two highest performing QH configurations. In both the Wistell-B and Ku5 configurations, strong indentations in the plasma boundary make designing coils extremely challenging (see for example fig 13 in [8]). However, coils that reproduce the energetic particle properties have already been designed for the Wistell-A configuration. The implication is that there is a trade-off between buidability and desirable properties. This trade-off is a subject of ongoing investigation.

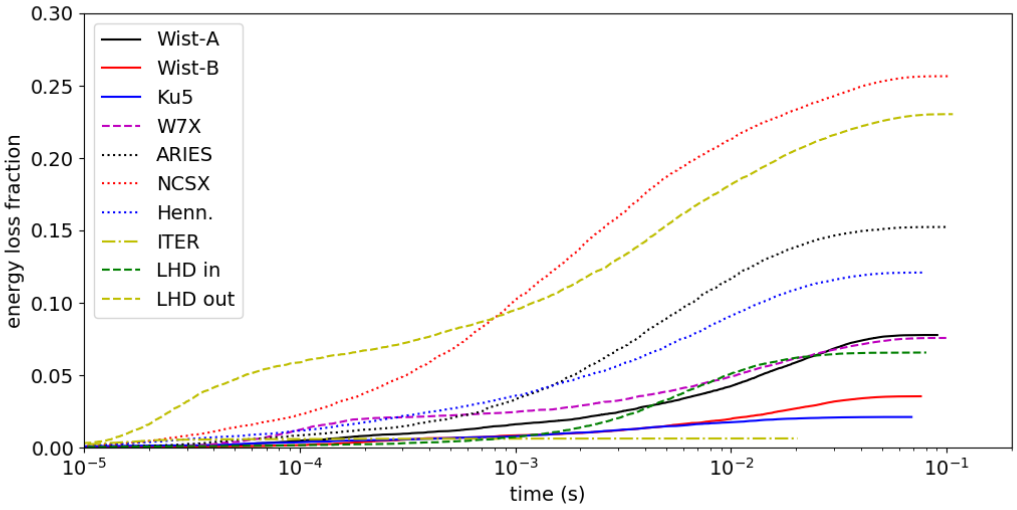

Figure 2: Alpha particle energy loss fraction as a function of time for 10 different configurations. QH configurations in solid lines, QA in dotted lines. Other stellarators are in dashed lines, and tokamaks are in dashed-dotted lines.

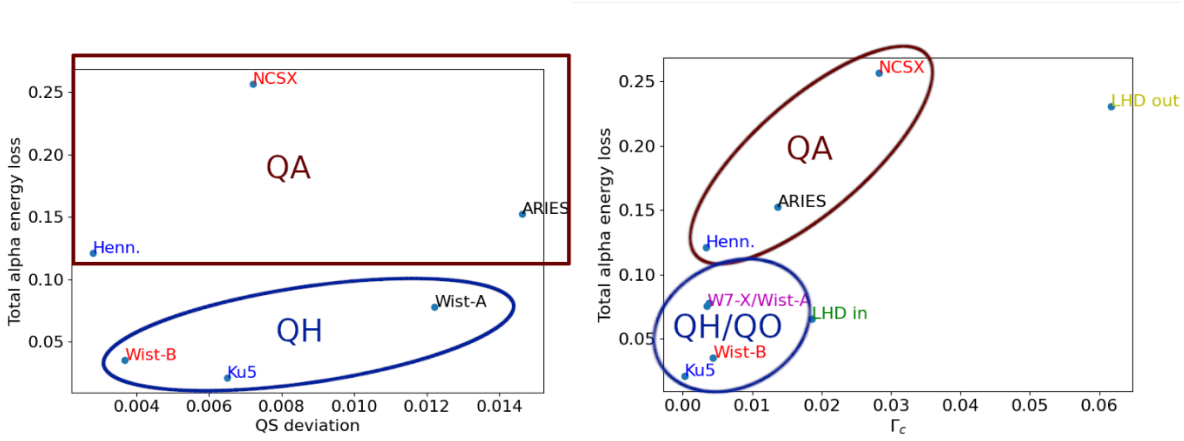

Figure 3: Total energy losses for configurations plotted against the minimum value of a specific figure of merit. Left: the figure of merit is the deviation from quasisymmetry. Only QH and QA configurations are included on this plot. Right: All stellarator configurations are plotted against the neoclassical metric, Γ_c.

The W7-X configuration was specifically designed for good energetic particle transport (ref from drev) and indeed it outperforms the QAs and is on par with the Wistell-A configuration for collisional calculations. Interestingly, the W7-X and Wistell-A configuration also have the same minimum value for Γc so the points overlap on Figure 3 right.

The inward shifted LHD-like configuration has properties that deserve some attention. The overall losses for this configuration are on par with both W7-X and Wistell-A. Even more interesting is that this configuration does exceedingly well at confining prompt losses. This good performance is despite not performing particularly well on the Γ_c metric.

Results from calculations without collisions help explain the performance of the LHD-like inward shifted configuration. Figure 4 shows the collisionless losses for all the configurations, when particles are sourced on the s=0.3 flux surface and followed without collisions. No particles are lost before 2 ms, outperforming the Wistell-A configuration which loses a few particles promptly. However, after long times most of the trapped particles escape the confined volume, with the total losses eventually equivalent to the trapped passing boundary. In the inward shifted LHD configuration, all the particles will drift out of the device, but they do it

very slowly. Furthermore, there are no orbits launched at s=0.3 that are promptly lost. When collisions are added to the calculation, most particles have ample time to deposit their energy before they are lost.

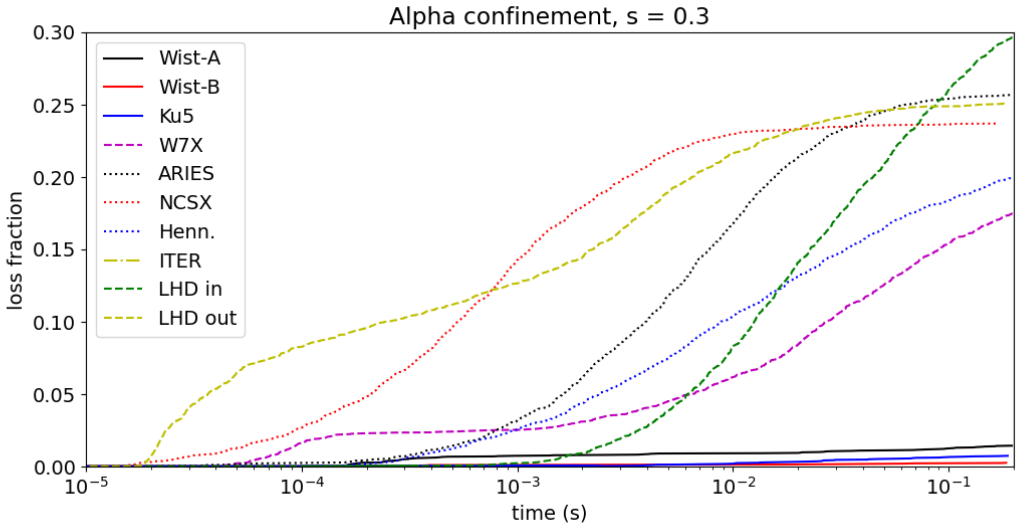

Figure 4: Collisionless alpha particle loss as a function of time for 10 different configurations. QH configurations in solid lines, QA in dotted lines. Other stellarators are in dashed lines. ITER is included in the legend but has no collisionless losses at this radius.

A striking result from the collisionless losses is how much better the QH configurations perform than the other configurations. While in general the QH configurations still outperform other configurations when collisions are added, the performance gap is narrower.

5. DISCUSSION

The broad survey of alpha particle confinement in stellarators has yielded some results which highlight the strengths and weakness of various configuration. The best performing configurations are QH configurations, but among these, the best performing QH configurations are ones that are very difficult to construct due to shaping. To date, it has not been possible to generate coils for the Wistell-B and Ku5 configurations that maintain excellent energetic particle. However, such coil designs have been successful for Wistell-A.

The proxy, Γ_c, appears to have some predictive capability for energetic particle confinement. Configurations that perform better on this metric tend to outperform other configurations of their type. Γ_c has also been useful as an optimization metric, and it was used to optimize both the Wistell-A and Wistell-B configurations.

Both QH, where contours of magnetic field strength close helically, and W7-X type configurations, where contours close poloidally have shorter connection lengths between bounce points than QA configurations, where contours close toroidally. These shorter connections lengths lead to smaller banana widths which could be one reason for the improved transport seen in these configurations. The good performance of the LHD inward shifted configuration may also be partly attributed to having low connection lengths. Even though most of the orbits are lost, even collisionlessly, the radial transport is sufficiently slow.

QH configurations are seen to perform extremely well in collisionless calculations. When collisions are included, they still perform well but the gap is significantly reduced. For a configuration like Wistell-A, collisionless calculations show only 2 out of 5000 particles are lost when started on the s=0.2 surface and followed for 0.2 s. However for W7-X, a full 13% of the particles are lost collisionlessly when started on the s=0.2 surface. Yet when collisions are added to the mix, W7-X and Wistell-A perform almost identically.

This result, along with the behavior of LHD prompts some thoughts on lost orbits in general. Some particles launched deep within the plasma are promptly lost in some configurations. This is evident when examining the NCSX or LHD outward shifted configurations. Ignoring the gyrophase, launched particles can be uniquely identified by four coordinates, three for the position in space and one for the pitch relative to the magnetic field. For each configuration there are areas in this 4D space that are confined (such as all passing particles) and areas that are lost. In some configurations there are areas of phase space that are promptly lost even in the core of the plasma. For this discussion we will consider a particle promptly lost if it is lost with 10^{-3} seconds. It is evident from the Monte-Carlo sampling that the prompt loss regions are more plentiful in some configurations than in others.

A typical feature of configurations with good confinement is seen by examining the magenta dashed curve in Figure 4, which is the W7-X configuration. Here, about 2% of the particles are promptly lost within 10^{-4} seconds. There are no additional losses between 10^{-4} and 10^{-3} seconds, after which losses start increasing. This type of behavior is also evident in collisionless calculations of QH cases, although the total numbers are too low to see in figure 4 except for the Wistell-A configuration. In these configurations some particles are lost promptly and any other losses arise from a very slow radial drift. Contrast that to LHD-inward (green dashed) in which no prompt losses occur before 10^{-3}. From this one can conclude, that at least at the resolution of the Monte Carlo sampling, there are no prompt loss orbits for the LHD inward shifted configuration, whereas there are for W7-X and Wistell-A.

When collisions are added, particles can diffuse through phase space by pitch-angle scattering. Although pitch-angle scattering is small for 3.5 MeV alpha particles compared to momentum loss, it still exists. If a particle diffuses into a region of phase space which is promptly lost, it will likely be lost before it can diffuse out. Furthermore, the distribution of the loss regions in phase space is important. If there is one major region of losses, such as all deeply trapped particles, the only particles that will be lost are those born in the region or close to it. However, if the prompt-loss regions are scattered around phase space, even if the total volume is lower, the amount of particles that may drift through a prompt-loss may be higher. Although verification will require statistical analysis tools beyond the scope of this paper, some basic analysis can be done by examining the pitches of promptly lost particles. Figure 5 shows a histogram of particle losses for W7-X and Wistell-A as a function of pitch. The pitch parameter is given as E/μ where E is the particle energy and μ is the first adiabatic invariant. This ratio is the maximum field a particle can reach before reflecting. The trapped-passing boundary is slightly different for the configurations but is roughly around 6.5 T for this flux surface. All the lost particles are trapped. Most of the losses from W7-X are from deeply trapped particles. While there are some losses near the trapped passing boundary for W7-X, there are fewer losses near the trapped-passing boundary for W7-X than Wistell-A.

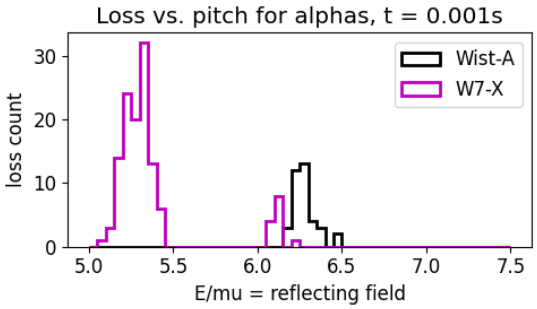

Figure 5: Total number of collisionlessly lost particles (out of 5000 launched) within 1 ms for Wistell-A (black) and W7-X (magenta) configurations. The x-axis represents the field a trapped particle will reflect at. The trapped passing boundary occurs at approximately 6.5 T for Wist-A and 6.3T for W7-X.

One explanation for the results is as follows. LHD-inward shifted has no prompt losses and the collisional results appear similar to the collisionless results. Most particles are lost, but they are lost slowly. W7-X does have prompt losses, but these occur mostly in the deeply trapped particles. Only particles that are close to the deeply trapped region can be lost. In contrast the losses from Wistell-A occur mostly near the trapped-passing boundary. Since it is easier to diffuse into loss regions near the trapped-passing boundary (a particle can diffuse from two directions in pitch) the losses are enhanced for Wistell-A when collisions are included. One result from this analysis is that if a configuration is to have prompt losses, it is far better to have them in deeply trapped regions.

The analysis presented here has some caveats which should be mentioned. The configurations shown are all idealized VMEC calculations. VMEC only considers good flux surfaces and magnetic islands or stochastic regions are not present. This limitation is mitigated somewhat because the large orbits of alpha particles may average over small regions of stochasticity. Calculations with more realistic fields are left for future work. All particle tracing is done in the guiding center approximation. Alpha particles have large gyroradii and this approximation may not be valid in all cases, especially in configurations with smaller minor radii. Finally, particles are considered lost if they pass beyond the penultimate surface in the VMEC equilibrium. In reality, particles may leave the confined plasma and reenter. This effect may be strongest in QA configurations which have the largest banana orbits, but could also be important in LHD. Finally the particle launch profiles presented here were not generated self consistently, but rather set to be the same for each configuration. Each configuration will have different transport properties and alpha particle energy depositions which will change the temperature and density profiles. As of now, it is difficult to forecast the transport properties of reactors, and no attempt has been made in this paper.

6. CONCLUSION AND OUTLOOK

Results for alpha particle calculations for various configurations were presented. The results indicate that it may be possible to optimize for different configurations. Possible optimization metrics of quasisymmetry and Γ_c appear to be successful and yield possible paths for optimization. Additionally, the inward shifted LHD-configuration which aligns the local minima of the magnetic field on a surface appears to produce configurations that are very successful at confining prompt losses.

Stellarator optimization often requires a tradeoff between multiple different criteria, of which energetic particle confinement is just a single one. Other metrics include bulk particle transport, amenability to generation by coils, stability, edge/divertor considerations, and many others. Furthermore, requirements on energetic particle confinement will depend on material and wall considerations. If it is possible to design walls to handle some flux from promptly lost alpha particles, then it may be appropriate to relax the alpha particle confinement constraint. However, if no prompt losses are permitted, the design space for stellarator reactors shrinks considerably. Yet results here show that it is in principle possible to eliminate prompt alpha particle losses altogether, if that is what is necessary.

REFERENCES

[1] NEMOV, V. V., et al. Phys. of Plas. **6.12** 4622-4632 (1999)
[2] BOOZER, A.H. Phys. of Fluids **25** (3) 520-521 (1982)
[3] CANIK, J.M., et al. PRL **98.8** 085002 (2007)
[4] HENNEBERG, S.A. et al Plas. Phys. Control. Fusion **62** 014023 (2020)
[5] BADER, A. et al. J. Plas. Phys. **85.5** (2019)
[6] NEMOV, V.V., et al. Phys. of Plas. **15.5** 052501 (2008)
[7] BADER, A. et al. J. Plas. Phys. **86.5** (2020)
[8] KU, L.P. and BOOZER, A.H. Nuc. Fus. **51** 013004 (2010)
[9] ZARNSTORFF, M.C., et al., Plas. Phys. Control. Fusion **43.12A** A237 (2001)
[10] KU, L.P. et al., Fus. Sci. and Tech. **54** 673-693 (2008)
[11] HENNEBERG, S.A., Nuc. Fus. **59.2** 026014 (2019)
[12] W7x ref
[13] MYNICK, H.E., Phys. of Fluids, **26.4** 1008-1017 (1983)
[14] TOBITA, K., et al., Plas. Phys. Control. Fusion **45.2** 133 (2003)
[15] HIRSHMAN, S.P., WHITSON, J.C. Phys. of Fluids **26.12** 3553-3568 (1983)
[16] MYNICK H.E., et al., Phys. of Plas. **13.6** 064505 (2006)